Study of lattice dynamics and phase transitions in betaine phosphate by comparison with betaine phosphite via infrared reflectivity spectroscopy

1997 J. Phys.: Condens. Matter 9 8119

(http://iopscience.iop.org/0953-8984/9/38/016)

J. Phys.: Condens. Matter **9** (1997) 8119–8134. Printed in the UK PII: S0953-8984(97)80643-1

Study of lattice dynamics and phase transitions in betaine phosphate by comparison with betaine phosphite via infrared reflectivity spectroscopy

M L Santos†, A Almeida†, M R Chaves†, A Klöpperpieper‡, J Albers‡, J A Gomes-Moreira† and F Gervais§‖

† Departamento de Fisica, Faculdade de Ciencias da Universidade do Porto, Praça Gomes Teixeira, P-4050 Porto, Portugal

‡ Fachbereich Physik der Universität der Saarlandes, D-6600 Saarbrücken, Germany

§ Centre de Recherches sur la Physique des Hautes Températures, CNRS, 45071 Orléans Cédex 2, France

Received 3 January 1997, in final form 23 May 1997

Abstract. The temperature dependence of infrared reflection spectra of betaine phosphate single crystal is reported for polarizations parallel to the *a*- and *b*-axes. The spectra were fitted with the factorized form of the dielectric function. A mode assignment is proposed on the basis of a comparison with the spectra of betaine phosphite and deuterated betaine phosphate. Some very asymmetric phonon lines are observed, and the importance of mode couplings is emphasized. A picture of a tendency towards transverse optical mode softening of the low-frequency spectrum upon approaching either side of the $T_2 = 86$ K phase transition temperature emerges for the polarization parallel to the *b*-axis, consistent with the peak observed in the temperature dependence of the dielectric constant. On the other hand, the temperature dependence of the ionic effective charges does not display any appreciable discontinuity at the phase transition, contrary to what is observed at the temperature of the transition to the ferroelectric phase of the parent compound betaine phosphite. This is consistent with the very low level of the spontaneous polarization below T_2 in betaine phosphate. The similarities of the behaviours with those of the compounds of the KDP family are discussed.

1. Introduction

Betaine phosphate (BP)—$(CH_3)_3NCH_2COOH_3PO_4$—and betaine phosphite (BPI)—$(CH_3)_3NCH_2COOH_3PO_3$—are addition compounds of the amino acid betaine and inorganic compounds of phosphorus and phosphoric acid, respectively. From BP and BPI aqueous solutions, single crystals of mixed $BP_{1-x}BPI_x$ have been obtained. This family of compounds, both pure and mixed, present a wide range of interesting and complex dielectric properties which have been the subject of extensive study in recent years. Similarly to what happens in some fairly well studied systems such as $NH_4H_2PO_4$, RbH_2PO_4, $NH_4H_2AsO_4$, and the mixed crystals $Rb_{1-x}(NH_4)_xH_2PO_4$, currently known as RADP, the protons of the O–H...O bonds play an important role in the low-temperature phase transitions, as can be seen in the effect of deuteration on the phase transition temperatures. And, just like for RADP, there have been found manifestations of frustration phenomena stemming

‖ Permanent address: Laboratoire d'Electrodynamique des Matériaux Avancés, Faculté des Sciences et Téchniques, Université François Rabelais, Parc de Grandmont, F-37200 Tours, France.

0953-8984/97/388119+16$19.50

from ferroelectric and antiferroelectric competitive interactions. $BP_{1-x}BPI_x$ presents a far more complex structure and dielectric behaviour (as will be summarized in the following), which makes it difficult to understand the mechanisms responsible for the different phase transitions. The inorganic groups (PO_4 in BP, PO_3 in BPI) are linked by hydrogen bonds, forming zig-zag-like chains along the [010] axis. The betaine molecules are oriented almost perpendicularly to the chains (along [001] directions) and are linked to the tetrahedra by one (BPI) or by two (BP) hydrogen bonds [1, 2]. Both BP and BPI crystallize in the monoclinic system [3–5]. In BP, the temperature evolution of the dielectric constant [3], polarization [3], and specific heat [6], as well as the x-ray patterns [7] and Raman [8] spectra, have revealed anomalies which have been related to three structural phase transitions occurring at the temperatures $T_1 = 365$ K, $T_2 = 86$ K, and $T_3 = 81$ K. At T_1, the system evolves from a paraelectric high-temperature phase with a $P2_1/m$ symmetry to an antiferrodistortive phase $P2_1/c$ with a simultaneous doubling of the unit cell along the c-axis [1, 3]. The phase transition at T_2 was detected on the basis of an anomaly in the dielectric constant [3]. The phases below T_2 were identified as antiferroelectric, as double hysteresis loops were obtained for fairly high ac electric fields [3]. This inference was not discredited by pyroelectric measurements on BP, which showed evidence of a very small polarization (in the nanocoulomb range) for $T < T_2$ [9], perhaps due to a small misorientation of the sample. But recent and very accurate x-ray diffraction measurements [7] lead to a different conclusion, by allowing the determination of the symmetry of the different low-temperature phases. In particular, the phase between T_2 and T_3 was found to have $P2_1$ symmetry, which indicates it to have a ferroelectric behaviour along $\boldsymbol{b}$. At T_3, a doubling of the unit cell occurs along the a-axis [10], and the low-temperature phase has a $P2_1/c$ symmetry.

BPI is known to present two structural phase transitions [7]: at $T_1 = 355$ K, from a paraelectric $P2_1/m$ high-temperature phase to an antiferrodistortive $P2_1/c$ phase with a simultaneous doubling of the unit cell along the c-axis and an order–disorder paraelectric phase transition to a $P2_1$ phase [11] occurring at 220 K. The existence of a soft relaxational mode associated with the latter transition is suggested by Koch and Happ in reference [12]. ENDOR measurements [11] established that the phase transition at T_2 is related to a dynamic proton order in the two hydrogen bonds linking each PO_3 group to its chain neighbours. A low-temperature glass-like phase has been proposed by some authors [13]. Deuteration raises T_2 by $\sim$70 K in BP [14] and by $\sim$100 K in BPI [15].

Further work on some mixed single crystals of $BP_{1-x}BPI_x$ using both macroscopic (complex dielectric constant and pyroelectric measurements) [9, 16–18] and microscopic techniques (x-rays) [7] resulted in the drawing of a phase diagram concerning the whole family $BP_{1-x}BPI_x$ in the range of variation of x from 0 to 1: for $0.90 < x < 1$ a transition occurs to a $P2_1$ ferroelectric phase; for $0 < x < 0.20$ the two successive transitions are to a $P2_1$ phase and subsequently to a Pc phase with a simultaneous doubling of the unit cell along the a-axis; and for $0.20 < x < 0.90$ we obtained clear evidence of an isomorphous transition to a glass phase and identified an orientational glass phase for $x = 0.80$. Evidence of the existence of a strong anisotropy for all of the concentrations studied was put forward [7]. The comparison between the weak anomalies found in the temperature dependence of the lattice parameters and the strong anomalies found in $\varepsilon(T)$ [7] shows that the ordering of the dipoles is not accompanied by significant lattice distortions.

Beginning with the study of BP, we will be looking for the identification of the relevant vibrational modes through the low transition temperatures, and will be studying the contribution of the interactions among the different force fields as well as the importance of the different couplings among the numerous vibrational modes of the lattice. This first step of a more complete study is a preliminary test of the feasibility of the method for

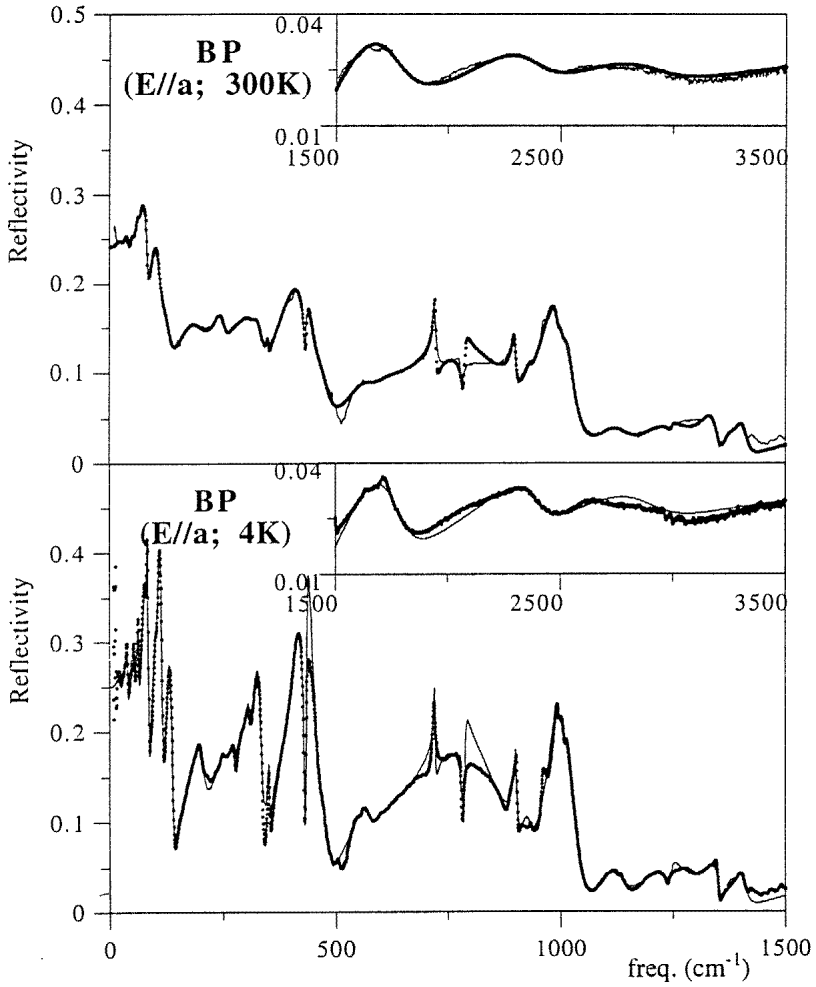

Figure 1. Examples of best fits of the dielectric function model equation (1) to infrared reflection spectra at the two extreme temperatures investigated, for the polarization parallel to the *a*-axis.

helping with comprehending complex systems. If the test is conclusive, it may open up new perspectives in the understanding of many systems which are little studied because they are considered too complex.

2. Sample preparation

Protonated and deuterated samples were obtained from high-quality single crystals grown from aqueous solution. In the growth process, while almost all protons in the H–O–H bridges are substituted for with deuterons, the ones in the betaine molecule are only replaced to a very small degree. After careful orientation of the mother crystal, the samples were cut and polished using distilled H_2O for the hydrogenated ones and D_2O for the deuterated ones. The polished faces so obtained showed good optical quality. Regarding the deuterated samples, special care was taken in polishing the relevant surfaces with D_2O immediately

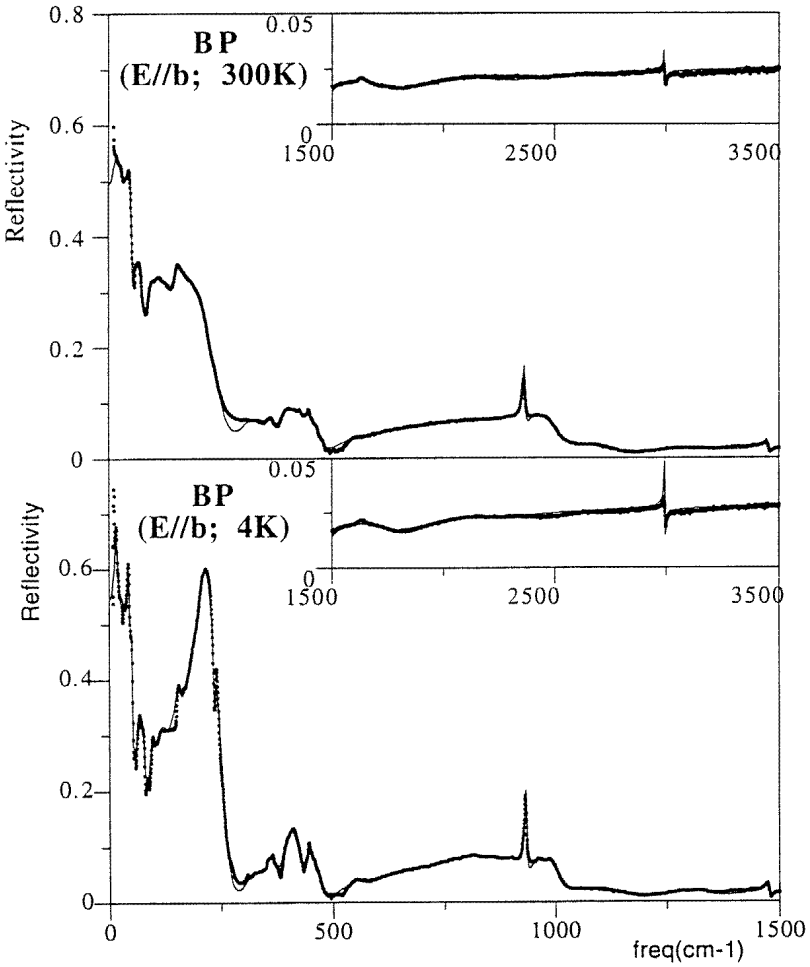

Figure 2. As figure 1, but for the polarization parallel to the *b*-axis.

before the setting in the cryostat, so minimizing the known effect of surface hydrogenation which is common in this type of material.

3. Infrared reflectivity spectroscopy

Anticipating the analysis which follows, it turns out that the absorption coefficient of betaine phosphate exceeds 1000 cm^{-1} in most of the spectral range of interest: 300–3000 cm^{-1}. This is due to the vibrations of phosphate groups coupled with those of O–H. . .O bonds. Such vibrations are more polar than those associated with covalent bonding inside the betaine molecule (see the structure pattern in figure 1). This means that, by using transmission spectroscopy, the relevant information could be obtained only with very thin platelets (thicknesses of 10 μm or even less) which would be difficult to prepare and to handle. It is therefore much more convenient to work using the reflectivity of thick crystal plates.

One platelet with a face of 9×7 mm containing the *a*- and *b*-axes was studied with a BRUKER IFS 307 Fourier-transform infrared spectrometer in the spectral range

Table 1. Tentative assignment of the vibrational modes in BP.

Frequency (cm^{-1})	Assignment
Internal modes of the betaine molecule	
2990	C–H stretching
2350	C–O stretching
1750	C=O
1460	N–C stretching (ν_3)
920	N–C bending (ν_4)
Internal modes of the phosphate tetrahedra	
800–900	Stretching (ν_3)
400–450	Bending (ν_4)

10–5000 cm^{-1}. The spectrometer is able to cover a wider range (10–42 000 cm^{-1}) but the limit retained in the spectra is sufficient and gives access to all of the relevant information for the present study. Spectra have been obtained between 4 K and 300 K with a variable-temperature cryostat equipped with interchangeable KRS5 and polyethylene windows. Spectra can then be Kramers–Kronig transformed to obtain the dielectric response. This treatment may be complemented by a fit of the dielectric function model

$$\varepsilon(\omega) = \varepsilon_\infty \prod_j \frac{\Omega_{jLO}^2 - \omega^2 + i\gamma_{jLO}\omega}{\Omega_{jTO}^2 - \omega^2 + i\gamma_{jTO}\omega} \tag{1}$$

to reflectivity data via

$$R(\omega) = \left| \frac{\sqrt{\varepsilon(\omega)} - 1}{\sqrt{\varepsilon(\omega)} + 1} \right|^2 . \tag{2}$$

In equation (1), the subscripts TO and LO refer to transverse and longitudinal optical modes, respectively. The Ωs represent frequencies and the γs mode dampings (the linewidth at half-maximum). The dielectric function model equation (1) is preferred to the more conventional summation over Lorentz oscillators for the reasons detailed in the review paper [19]. In particular, the factorized form of the dielectric function was successfully used to fit the spectra of compounds displaying the parent properties, e.g. RbDP [20–22]. For the specific case of BP (and BPI too), the model equation (1) appears to be the simplest one which is able to fit the data satisfactorily. Indeed, we will see that certain regions of the spectra display heavily damped modes—internal to the PO_4 tetrahedra—strongly coupled with proton motions, alternating with very narrow lines of the betaine molecules. As a result, since all TO modes are coupled as will be detailed below—and LO modes equally well—two neighbouring TO and LO oscillators may exhibit very different damping terms γ. This is just the situation in which the factorized form of the dielectric function equation (1) is the most useful, because it does not implicitly assume the same damping for two neighbouring TO and LO modes as the more usual summation model does, as explained in reference [19]. In particular, this situation may give rise to very asymmetric phonon lines that result from the coupling of a narrow line with a broad continuum, and the factorized form, equation (1), is able to describe the line profiles satisfactorily in this case, as shown in references [20–22] for example.

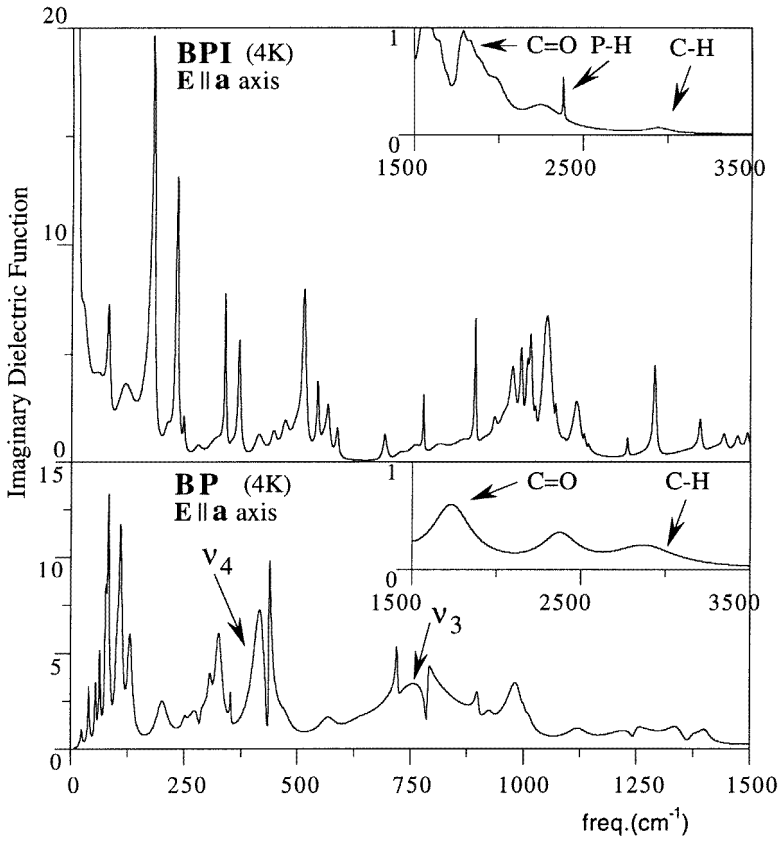

Figure 3. A comparison of the imaginary part of the dielectric function of betaine phosphate (BP) and phosphite (BPI) showing the response of the transverse optical modes for the polarization parallel to the *a*-axis. The labels ν_3 and ν_4 refer to the internal modes of the phosphate tetrahedra.

4. Experimental results and discussion

4.1. Data fitting and mode assignment

Infrared reflection spectra for the polarization parallel to the *a*- and *b*-axes are shown in figures 1 and 2 for both of the extreme temperatures investigated. Spectra at five intermediate temperatures have been also recorded. All of the reflectivity spectra have been fitted with equations (1) and (2). Examples of agreement between the model and the experiment are shown in figures 1 and 2. The discussion of the case for BPI that is under investigation by the same procedure will be published later. However, for the present purposes, it is instructive to compare the spectra of BP and BPI to deduce a tentative assignment of the vibrational modes based on the fact that modes internal to the betaine molecule are expected to be little affected by the crystal field. The TO modes of both compounds at 4 K are compared in figures 3 and 4 for polarizations $\boldsymbol{E} \parallel \boldsymbol{a}$ and $\boldsymbol{E} \parallel \boldsymbol{b}$. The function displayed in figures 3 and 4 is the imaginary part of the dielectric response deduced from the best fit to the reflectivity spectra. Furthermore, a comparison of the results for BP with preliminary results obtained for partially deuterated BP, here labelled DBP, is shown in figures 5 and 6. The comparison is made with Kramers–Kronig-transformed DBP data. The complexity

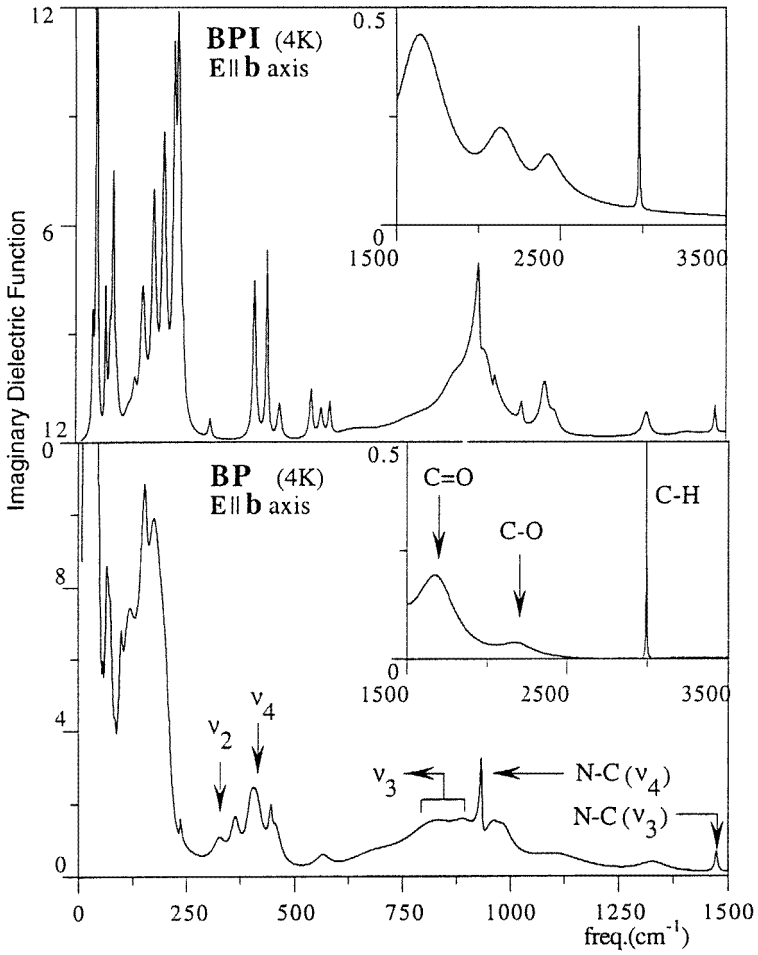

Figure 4. As figure 3, but for the polarization parallel to the *b*-axis.

of the results probably means that not only are the protons of the inorganic tetrahedra substituted for with deuterons, but also the protons of the betaine molecules are partially substituted for with deuterons. Another possibility—that is supported by what follows—is that the proton (or deuteron) motions are strongly coupled with vibrations of atoms belonging to PO_4 tetrahedra, and also with C=O and C–O vibrations. The comparison of our data with other published data, in particular infrared spectra of a tetramethylammonium compound previously investigated by one of us [23] and which consists of N–$(CH_3)_4$ tetrahedra fairly similar to those in the central part of the betaine molecule, allows us to tentatively propose the mode assignments summarized in table 1 and reproduced in figures 3–6. O–H. . .O stretching modes are expected to lie within the same range as C–O and C–H vibrations, as observed in parent KDP and DKDP compounds, and this probably explains the additional bumps in this spectral region. The groups of bands which may be safely assigned are the stretching (ν_3) and bending (ν_4) vibrations of both PO_4 and N–$(CH_3)_4$ tetrahedra. The assignment of the C–H vibrations near 2990 cm^{-1} is also straightforward. In the present state of knowledge of the data, it would be hazardous to claim more about

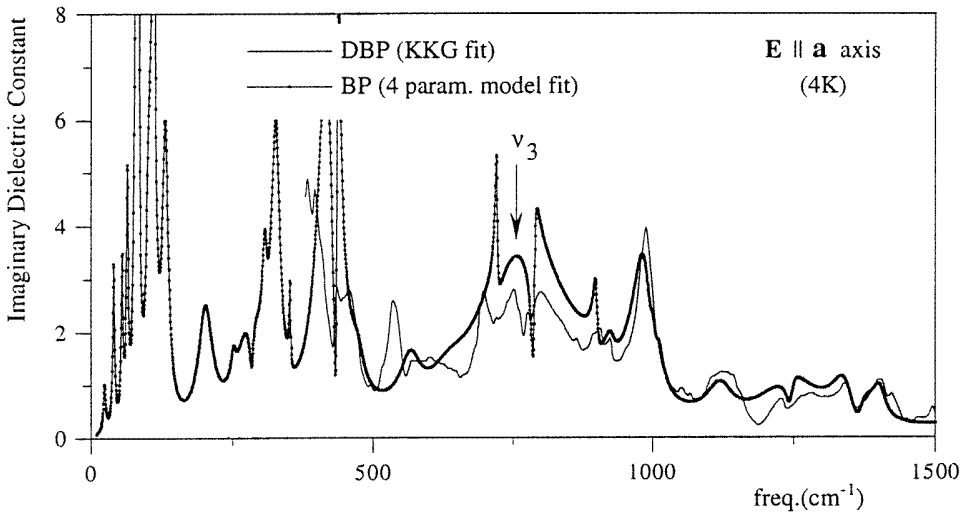

Figure 5. A comparison of hydrogenated and deuterated betaine phosphate for the polarization parallel to the *a*-axis.

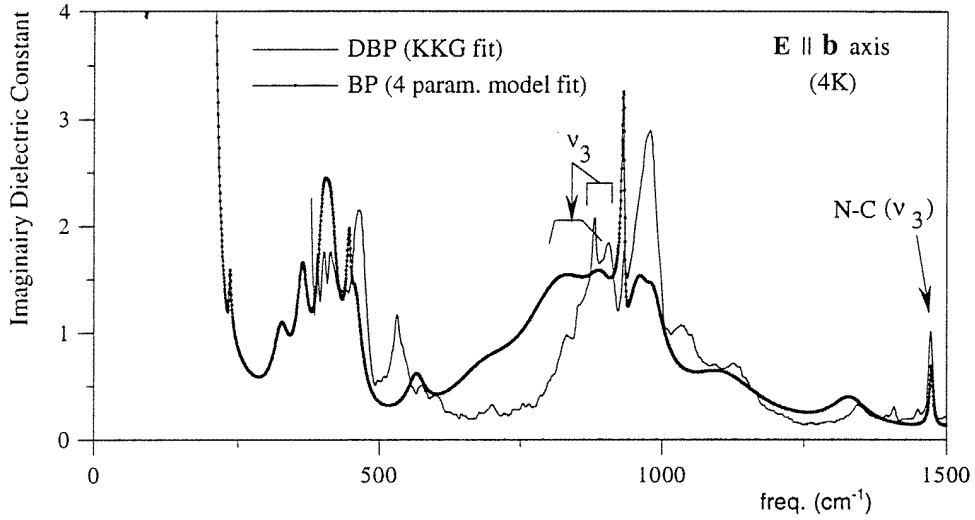

Figure 6. As figure 5, but for the polarization parallel to the *b*-axis.

mode assignments without having complementary information from parent systems. These assignments nevertheless are sufficient for the purposes of this paper.

The results obtained from a factor group analysis of BP in different phases are summarized in table 2. We observe that the number of infrared-active modes below T_1, for both polarizations, $\boldsymbol{E} \parallel \boldsymbol{a}$ and $\boldsymbol{E} \parallel \boldsymbol{b}$, is predicted to be equal to or greater than 82. The number of modes used in the fit of the reflectivity data below T_1, typically 40 modes, is always lower than the corresponding one calculated from group theory analysis. The good fits obtained seem to indicate that the infrared-active modes that are not considered play a less important role in the infrared spectra of BP, probably because they are too weakly polar.

Table 2. Factor group analysis of the various phases of BP and optical mode activities.

$T_1 = 365$ K			$T_2 = 86$ K			$T_3 = 81$ K					
$P2_1/m$			$P2_1/c$			$P2_1$			$P2_1/c$		
Number of modes	Species	Optical activity	Number of modes	Species	Optical activity	Number of modes	Species	Optical activity	Number of modes	Species	Optical activity
45	A_g	R	78	A_g	R	161	A	R, IR	156	A_g	R
33	B_g	R	78	B_g	R				156	B_g	R
35	A_u	IR	83	A_u	IR	160	B	R, IR	166	A_u	IR
46	B_u	IR	82	B_u	IR				164	B_u	IR

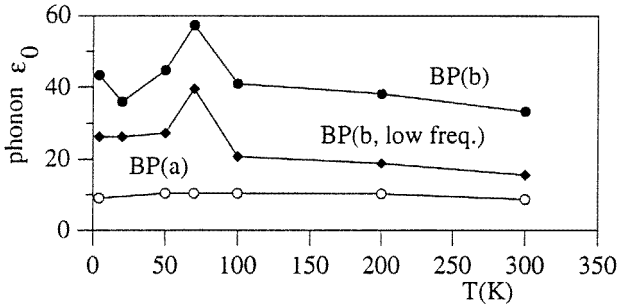

Figure 7. A comparison of the temperature dependences of the sums of oscillator strengths of infrared phonon modes for the polarizations parallel to the *a*- and *b*-axes. Note that the peak at T_2 for the polarization parallel to $\boldsymbol{b}$ is explained by the temperature dependence of the sum of the lowest three frequency modes.

4.2. Mode coupling, oscillator strengths, and the dielectric constant

In all of the spectra that consist of more than one excitation, the modes are coupled, the more so as they become nearer in frequency. There are two extreme limit behaviours of the mode coupling: (i) discrete mode–mode coupling which manifests itself in level repulsion phenomena; and (ii) interference of a discrete state with a broad continuum. The signature of the latter case is generally a strong asymmetry of the narrow line, which may appear as a hole in the continuum instead of a peak in extreme cases, and is well described by the general Fano formalism [23]. Upon inspection of the results obtained at 4 K in figures 3 and 4, the striking feature is the existence of narrow and broad bands that interfere to give asymmetric profiles as shown for the ν_3 and ν_4 PO_4 mode groups. We additionally checked that the model equation (1) fits the data satisfactorily, including those for the very unconventional PO_4 ν_3-mode region for $\boldsymbol{E} \parallel \boldsymbol{a}$ (figure 3), and describes the highly asymmetric line profiles correctly. Similar broad profiles were observed in KDP-type crystal spectra. They were understood in terms of the coupling of proton motions in the hydrogen bridges with internal degrees of freedom of the PO_4 tetrahedra [20–22]. This interpretation was substantiated by the observation of coupled-proton ν_4-mode softening that triggers the PE–FE phase transition. Here we observe that the wavenumber range in which at least some modes display unusual broadening extends up to 2500 cm^{-1} for $\boldsymbol{E} \parallel \boldsymbol{b}$ and 3500 cm^{-1} for $\boldsymbol{E} \parallel \boldsymbol{a}$, even at 4 K. This spectral range is compatible with proton motions—vibrational or relaxational—owing to the low proton mass.

Before proceeding to extract relevant information from the spectra, it is instructive to

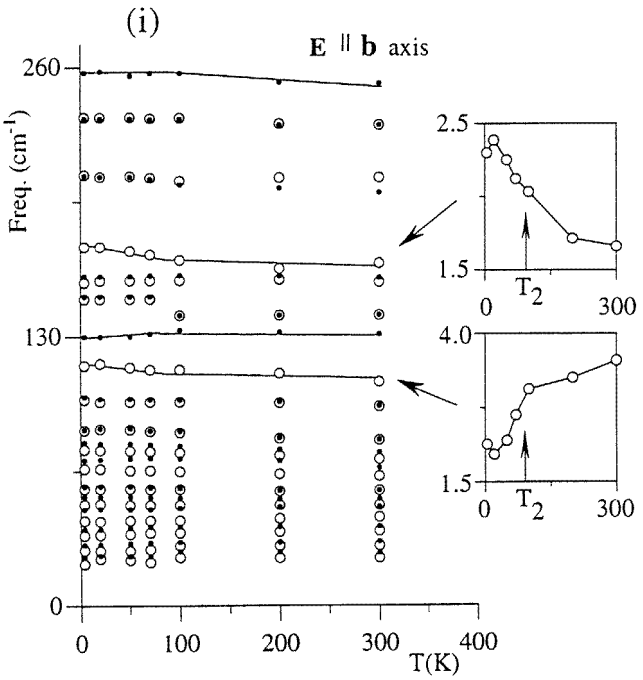

Figure 8. The temperature dependence of the TO (open symbols) and LO (full symbols) modes in betaine phosphate for the polarization parallel to the *b*-axis. The insets show the temperature dependence of the dielectric strength of the corresponding TO modes $\Delta\varepsilon_j$, related to the TO and LO mode frequencies via equation (3).

inspect the temperature dependence of the dielectric constant at 10 cm^{-1} (300 GHz), which is the low-frequency limit of our spectra. It is obtained as $\varepsilon_0 = \varepsilon_\infty + \sum \Delta\varepsilon_j$ by summing over ε_∞ and all individual oscillator strengths $\Delta\varepsilon_j$ evaluated via

$$\frac{\Delta\varepsilon_j}{\varepsilon_\infty} = \Omega_{jTO}^{-2}\left(\prod_k (\Omega_{kLO}^2 - \Omega_{jTO}^2)\right)\Big/\left(\prod_{k\neq j} (\Omega_{kTO}^2 - \Omega_{jTO}^2)\right) \tag{3}$$

or equally well on setting $\omega = 0$ in equation (1) and using the generalized Lyddane–Sachs–Teller relationship

$$\varepsilon_0 = \varepsilon_\infty \prod_j \frac{\Omega_{jLO}^2}{\Omega_{jTO}^2}. \tag{4}$$

The temperature dependence of ε_0 at 300 GHz is plotted in figure 7 for both of the polarizations studied. No anomaly is found parallel to the *a*-axis, whereas a peak compatible with the position of the T_2 phase transition is evident parallel to the *b*-axis. Note that the magnitude of ε_0 (300 GHz) observed parallel to $\boldsymbol{b}$ at T_2 is only 30% of the static dielectric constant measured at 10 kHz, and does not explain the higher values obtained at higher temperature, the maximum near 100 K in particular ($\varepsilon_0 = 485$) [3]. Other contributions lying at frequencies below 300 GHz must therefore exist. On the other hand, the temperature dependence of the phonon contribution is compatible with the magnitude of the small anomaly just at T_2. Inspection of the temperature dependence of the oscillator strength of each mode does not allow us to find one specific mode which is responsible

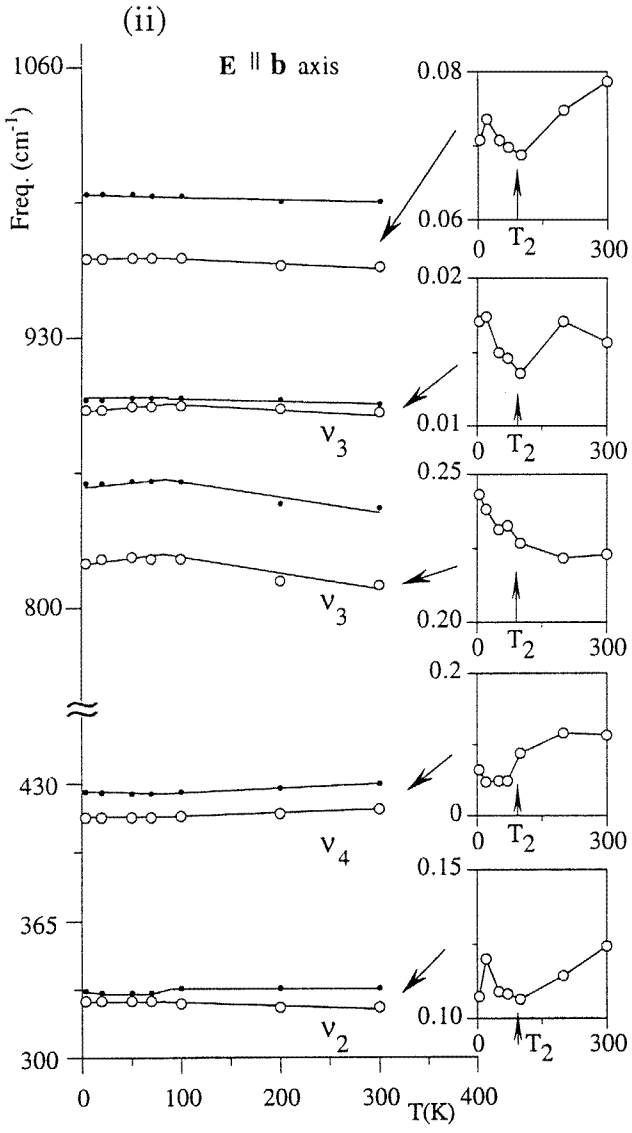

Figure 8. (Continued)

for the behaviour of ε_0 (300 GHz). Rather, a number of modes contribute, and the lower the frequency of the mode, the larger its contribution, on average. This is illustrated by the temperature dependences of the sums of the oscillator strengths of the three lowest-frequency modes, as can be seen in figure 7, which explains the observed dependence of ε_0 for the polarization parallel to the *b*-axis. Due to the large number of modes spread over a wide wavenumber range, mode couplings prevent us from identifying a single soft mode (by 'mode couplings', we mean both of the mechanisms (i) and (ii) recalled at the beginning of section 4.2). Rather, a general tendency towards softening upon cooling in the high-temperature phase and a mode hardening upon further cooling below T_2 is evident.

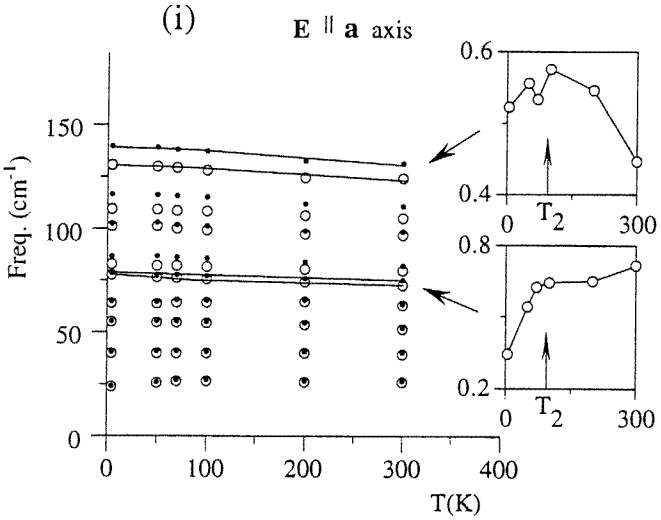

Figure 9. As figure 8, but for the polarization parallel to the *a*-axis.

This behaviour is more easily visualized by inspection of the oscillator strengths rather than observing the temperature dependence of the frequencies. They are shown as insets in figures 8 and 9. A number of mode oscillator strengths definitely show a more or less marked anomaly at T_2 in their behaviour. But some modes display a frequency maximum at T_2 while a minimum would be compatible with the behaviour of ε_0! The balance is necessarily positive, nevertheless, since ε_0 (300 GHz) shows a peak at or near T_2. These tendencies illustrate that most modes appear to be somewhat coupled to the order parameter of the phase transition. Among the modes which show a tendency towards softening (probed via a maximum of the oscillator strength and a minimum of the TO frequency at T_2), we note the ν_4 modes internal to the PO_4 tetrahedra (whereas ν_3 modes, for example, show an opposite behaviour). This observation emphasizes the similarity to phenomena already studied for the KDP family [20–22]. The tendency towards spectral broadening up to high frequencies suggests that proton motions lie at the origin of the mode softening. The instability of the proton motions, coupled with the phosphate internal modes, seems therefore also to couple with the external modes (phosphate tetrahedra against the betaine molecule) which have the lowest frequencies and are the main contributors to the dielectric constant.

4.3. Phase transitions

The results given in figures 8 and 9 show that no additional mode is reported below T_2 or T_3. We do not claim however that there is no additional mode—simply that the mode oscillator strength is too weak for us to be able to decide whether they disappear exactly at the phase transition or whether the natural broadening with temperature explains why they are hardly observable at room temperature. In other words, we did not plot them in figures 8 and 9, because their description in terms of frequency and damping parameters would imply insufficient accuracy. This result is consistent with the very small degree of spontaneous polarization which is observed below T_2 [9], and the small anomalies found in the temperature dependence of the x-ray diffraction [7]. It also confirms that the phase transitions involve very small atomic displacements which, in return, involve weak

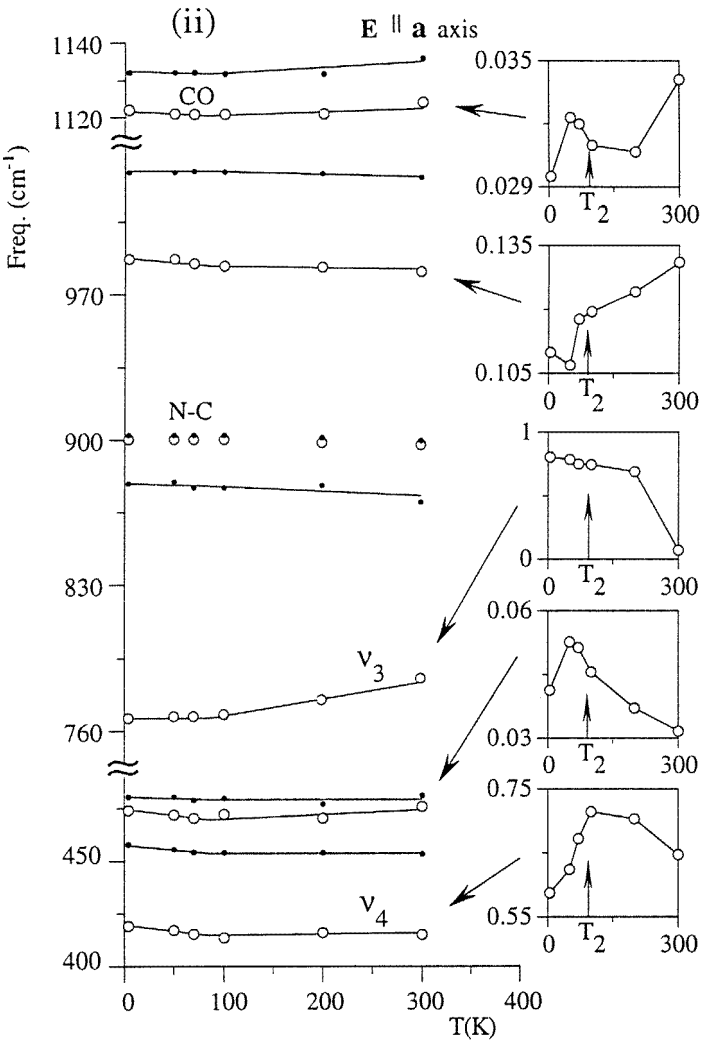

Figure 9. (Continued)

additional polar character (remember that only polar modes are probed by the infrared). The main signature of the phase transition that we observe rests on the many individual behaviours exhibited in figures 8 and 9, indicating coupling with an order parameter, and their cumulative effect, which shows up in the behaviour of figure 7.

5. Temperature dependence of ionic effective charges

Another advantage of infrared reflectivity spectroscopy lies in the availability of both TO and LO mode frequencies, which allow the determination of ionic effective charges $(Ze)_k$ that

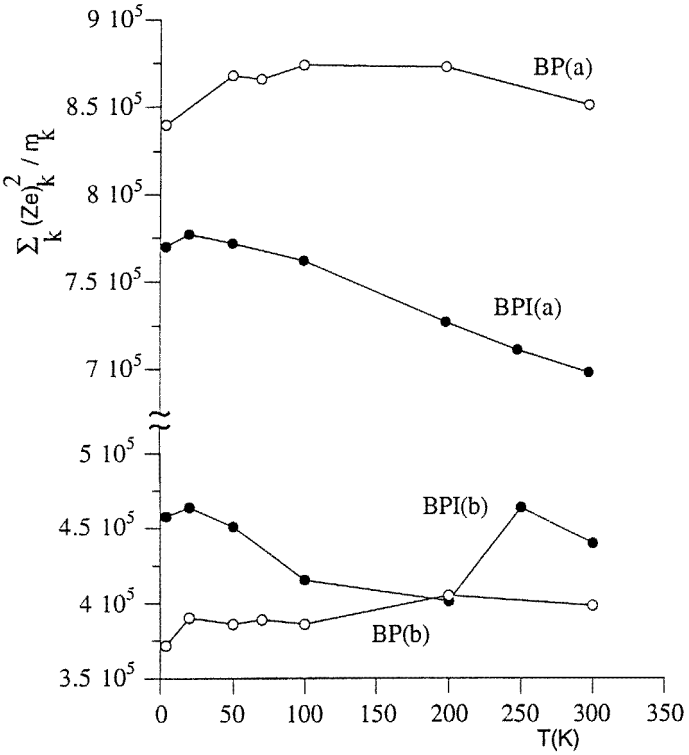

Figure 10. A comparison of the temperature dependences of a term related to the effective charges for $\boldsymbol{E} \parallel \boldsymbol{a}$ and $\boldsymbol{E} \parallel \boldsymbol{b}$ polarizations, and for BP and BPI. A marked discontinuity is observed at the Curie temperature for the polarization parallel to the ferroelectric axis of BPI only, consistent with the cation–anion pairing lying at the origin of the spontaneous polarization, and as observed for other ferroelectrics in the past.

are the origin of the instantaneous dipole moments probed by infrared radiation, via [24, 25]:

$$\sum_j (\Omega_{jLO}^2 - \Omega_{jTO}^2)_\alpha = \frac{1}{\varepsilon_V V} \sum_k \frac{(Ze)_{k_\alpha}^2}{m_k} \tag{5}$$

where α denotes a direction of polarization, and where the summation in the right-hand side of the equation is over all atoms of mass m_k contained in the unit cell of volume V. In all of the displacive ferroelectrics that one of the authors (FG) has investigated in the past, a decrease of Z in the direction parallel to the ferroelectric axis has been observed [26] (see references [21] and [22]), due to the pairing of cations and anions which are responsible for the spontaneous polarization in the ferroelectric phase. The temperature dependence of $\sum (Ze)_k^2/m_k$ is plotted in figure 10 for both of the polarizations studied for BP. Neither an obvious discontinuity nor a change of regime is observed within experimental error. This is consistent with the observations summarized at the end of the previous section, indicating a small displacement of ions at the phase transition and a very weak spontaneous polarization. By comparison, the situation contrasts with that for BPI, where a net decrease of the term $\sum (Ze)_k^2/m_k$ parallel to the FE b-axis is observed just below the PE–FE phase transition T_2, as shown in figure 10.

6. Summary

The temperature dependence (4–300 K) of the infrared reflection spectra of betaine phosphate single crystal has been reported for the polarizations parallel to the *a*- and *b*-axes over the wavenumber range 10–5000 cm^{-1}. The spectra were fitted with the factorized form of the dielectric function, satisfactorily. It was deemed important to check prior to future work on mixed crystal systems that such complex spectra containing very asymmetric spectral profiles may be fitted correctly with the simple phenomenological model equation (1). A tentative mode assignment has been proposed on the basis of a comparison with the spectra of betaine phosphite and deuterated betaine phosphate.

Asymmetric phonon lines have been observed. The asymmetries are currently understood in terms of mode couplings. The mode coupling phenomenon, which is found to be highly efficient in this compound, manifests itself by means of several signatures which emerge from the data and their analysis: (i) some very asymmetric narrow lines; and (ii) transfers of mode characteristics (frequency, dielectric strength, damping) that prevent an individual mode from displaying the usual behaviour, because it is no longer an individual mode but is now a mixed coupled mode. The phenomenon is particularly spectacular for modes which are suspected of being coupled to (supposedly broad) proton modes. Indeed, as in KDP-type spectra, the proton mode is not observed here as an individual excitation, but only via coupled and broadened modes. It is checked that the modes which are the most affected by the coupling with proton motions are internal to PO_4 tetrahedra, like in KDP-type systems. The limits of the tentative mode assignment are a straightforward consequence of mode couplings.

A picture of the tendency towards transverse optical mode softening of the low-frequency part of the spectrum (external modes) upon approaching either side of the phase transition temperature T_2 emerges for the polarization parallel to the *b*-axis, consistent with the small peak observed in the temperature dependence of the dielectric constant. On the other hand, the temperature dependence of the ionic effective charges does not display any appreciable anomaly at the phase transition, contrary to what is observed at the temperature of the transition to the ferroelectric phase of the parent compound betaine phosphite. This is consistent with the very low degree of spontaneous polarization below T_2 in betaine phosphate.

Acknowledgments

The authors thank Annie Blin and Albano Costa for technical assistance. FG thanks Dr P Simon for valuable discussions. This work was partially supported by the Service Culturel Scientifique et de Coopération de l'Ambassade de France au Portugal, by the Junta Nacional de Investigaçâo Cientifica e Tecnologica, by the Instituto de Materiais (IMAT-nucleo IFIMUP), and by Projecto Praxis XXI/2/2.1/FIS/26/94. J Agostinho Moreira thanks Programa Praxis XXI for grant BD/3192/94.

References

[1] Schildkamp W and Spilker J 1984 *Z. Kristallogr.* **168** 159
[2] Fehst I *et al* 1993 *Ferroelectrics* **138** 1
[3] Albers J, Klöpperpieper A, Rother H J and Ehses K H 1982 *Phys. Status Solidi* a **74** 553
[4] Albers J, Klöpperpieper A, Müser H E and Rother H J 1984 *Ferroelectrics* **54** 45
[5] Albers J, Klöpperpieper A, Rother H J and Haussühl S 1988 *Ferroelectrics* **81** 27

[6] Maeda M 1988 *J. Phys. Soc. Japan* **57** 3059
[7] Santos M L, Kiat J M, Almeida A, Chaves M R, Klöpperpieper A and Albers J 1995 *Phys Status Solidi* b **189** 371
[8] Freitag O, Brückner H J and Unruh H G 1985 *Z. Phys.* B **61** 75
[9] Santos M L, Azevedo J C, Almeida A, Chaves M R, Pires A R, Müser H E and Klöpperpieper A 1990 *Ferroelectrics* **108** 363
[10] Hayase S, Koshiba T, Terauchi H, Maeda M and Suzuki I 1989 *Ferroelectrics* **96** 221
[11] Bauch H, Böttcher R and Völkel G 1993 *Phys. Status Solidi* b **179** K41
[12] Koch G and Happ H 1993 *Ann. Phys., Lpz.* **2** 522
[13] Ebert H, Lanceros-Mendez S, Schaack G and Klöpperpieper A 1995 *J. Phys. C: Solid State Phys.* **7** 9305
[14] Brückner H J, Unruh H G, Fischer G and Genzel L 1988 *Z. Phys.* B **71** 225
[15] Santos M L 1997 to be published
[16] Santos M L, Chaves M R, Almeida A, Müser H E, Klöpperpieper A and Albers J 1993 *Ferroelectr. Lett.* **15** 17
[17] Hutton S L, Fehst I, Böhmer R and Loidl A 1992 *Ferroelectrics* **127** 279
[18] Ries H, Böhmer R, Fehst I and Loidl A 1996 *Z. Phys.* B **99** 401
[19] Gervais F 1983 *Infrared and Millimeter Waves* vol 8, ed K J Button (New York: Academic) pp 279–339
[20] Simon P and Gervais F 1985 *Phys. Rev.* B **32** 468
[21] Gervais F and Simon P 1987 *Ferroelectrics* **72** 77
[22] Simon P, Gervais F and Courtens E 1988 *Phys. Rev.* B **37** 1969
[23] Fano U 1961 *Phys. Rev.* **124** 1866
[24] Gervais F and Arend H 1983 *Z. Phys.* B **50** 17
[25] Gervais F 1976 *Solid State Commun.* **18** 191
[26] Gervais F 1980 *Phys. Status Solidi* b **100** 337
Gervais F 1981 *Phys. Rev.* B **23** 6580
Gervais F and Servoin J L 1981 *J. Physique Coll.* **42** C6 415
Fontana M D, Métrat G, Servoin J L and Gervais F 1984 *J. Phys. C: Solid State Phys.* **16** 483
Gervais F, Simon P, Echegut P and Calès B 1985 *Japan. J. Appl. Phys. Suppl.* 2 **24** 117